Phonon universal-transmission fluctuations and localization in semiconductor superlattices with a controlled degree of order

Norihiko Nishiguchi and Shin-ichiro Tamura
Department of Engineering Science, Hokkaido University, Sapporo 060, Japan

Franco Nori
Department of Physics, The University of Michigan, Ann Arbor, Michigan 48109-1120
(Received 25 February 1993; revised manuscript received 6 August 1993)

We study both analytically and numerically phonon transmission fluctuations and localization in partially ordered superlattices with correlations among neighboring layers. In order to generate a sequence of layers with a varying degree of order we employ a model proposed by Hendricks and Teller as well as partially ordered versions of deterministic aperiodic superlattices. By changing a parameter measuring the correlation among adjacent layers, the Hendricks-Teller superlattice exhibits a transition from periodic ordering, with alternating layers, to the phase-separated opposite limit, including many intermediate arrangements and the completely random case. In the partially ordered versions of deterministic superlattices, there is short-range order (among any N consecutive layers) and long-range disorder, as in the N-state Markov chains. The average and fluctuations in the transmission, the backscattering rate, and the localization length in these multilayered systems are calculated based on the superlattice structure factors we derive analytically. The standard deviation of the transmission versus the average transmission lies on a *universal* curve irrespective of the specific type of disorder of the superlattice. We illustrate these general results by applying them to several GaAs-AlAs superlattices for the proposed experimental observation of phonon universal-transmission fluctuations.

I. INTRODUCTION

For a long time, electronic devices were made of a single semiconductor material. This is no longer the case. Epitaxy and heterostructures have brought a revolution in device technology by placing different semiconductors, with different physical properties (dielectric constants, energy gaps, etc.), within distances of a few nanometers. For example, different lattice sizes in different adjacent semiconductors produce strain in the heteroepitaxy, altering its physical properties. Furthermore, recent developments in the technology for stacking different semiconductors, in order to fabricate multilayered thin-films, makes possible the realization of various semiconducting superlattices (SL's) with artificially imposed one-dimensional (1D) order in the growth direction. Specifically, in addition to the usual periodic stacking of semiconductors, several aperiodic multilayers have been fabricated, including quasicrystalline, Thue-Morse, and random superlattices. Their physical properties have been studied by a variety of experimental probes, including x-ray and Raman scattering. For a review on these topics, with further references, the reader is referred to Ref. 1. We note that the experimental studies of acoustic wave propagations (of both phonon and ultrasonic regimes) in some of these aperiodic systems have also been done by several groups.[2,3]

It is the purpose of this work to study systematically the phonon transport properties of superlattices as a function of their structural order. In particular, we study, both analytically and numerically, the transmission fluctuations and localization properties of phonons in two types of partially ordered SL's, which are described in more detail in the next two sections. The first type is based on the Hendricks-Teller (HT) model[4] for layered systems, which has the very convenient feature of having a tunable degree of structural correlation among neighboring layers. In particular, we consider the gradual and systematic transition from a periodic arrangement of alternating layers to the opposite, phase separated, regime and follow the corresponding changes in the transport properties induced by the changing structural order of the SL. The second type is based on the so-called three- and four-state Markov structures[5] and is illustrated with two examples, which are partially ordered versions[6] of the quasicrystalline[7,2] (QC) and Thue-Morse (TM) SL's.[8] It should be noted that the random version of QC SL's as defined by a three-state Markov process were also fabricated and the Raman spectra in these systems have already been measured.[1]

Our strategy is the following: we derive analytical expressions of I_s, the average phonon intensity reflected from the interface of layers, for several SL's with a varying degree of short-range correlations. From I_s, we analytically derive the localization lengths, transmission rate, and transmission fluctuations, all of which coincide well with the numerical results we obtain from the alternative transfer matrix method. The relation between the different quantities which characterize phonon trans-

port is presented. For instance, the Lyapunov exponent, which provides the inverse of the phonon localization length, is the logarithmic decrement of the transmission coefficient averaged over the realizations of disorder. We apply the general ideas and results derived here to several particular realizations of GaAs-AlAs SL's which are readily accessible experimentally. Our predictions for the universal phonon transmission fluctuations can be tested using currently existing experimental techniques in phonon spectroscopy and phonon imaging which have so far been used to verify the existence of phonon filtering actions of periodic and QC SL's.[2,9–12] The analogies and differences with the universal conductance fluctuations for transport in disordered systems[13] and speckle phenomena[14] will also be discussed.

In Secs. II and III, we describe in detail the two families of superlattices considered here. In Sec. IV, the phonon backscattering rate is studied in terms of the structure factors of the SL's, which we derive in closed form. Section V is devoted to the average transmission, transmission fluctuations, and the Lyapunov exponent. We illustrate in Sec. VI our general results by applying them to several proposed GaAs-AlAs superlattices, for the experimental observation of phonon transmission fluctuations. Section VII presents a summary of our results.

II. HENDRICKS-TELLER SUPERLATTICES

Consider a SL with two kinds of layers, hereafter denoted by A and B, occurring with frequencies f_A and f_B ($f_A + f_B = 1$, $f_A \geq f_B$). To introduce a correlation, consider two adjacent layers and denote by Q_{AA} the probability that layer A is followed by layer A, Q_{AB} the probability that A is followed by B, and so on. The first layer of the pair is A (B) with probability f_A (f_B); thus

$$Q_{AA} + Q_{AB} = f_A, \qquad Q_{BA} + Q_{BB} = f_B, \tag{1}$$

and similarly

$$Q_{AA} + Q_{BA} = f_A, \qquad Q_{AB} + Q_{BB} = f_B\ . \tag{2}$$

From Eqs. (1) and (2) we find

$$Q_{AA} = f_A - 1/4 + q, \qquad Q_{BB} = f_B - 1/4 + q,$$
$$Q_{AB} = Q_{BA} = 1/4 - q, \tag{3}$$

where $1/4 - f_A < q < 1/4$ and q measures the degree of correlation among adjacent layers. Note that for $f_A = f_B = 1/2$, $q = 0$ (i.e., no correlation) corresponds to the completely disordered case. Let $P_{AB} = Q_{AB}/f_A$ be the probability that the second layer of the pair is B if layer A is now introduced as the first layer of the pair. This conditional probability can be defined for any pair of layers (e.g., P_{BA}). For convenience, we also introduce $P_{(AA|B)}$ describing the conditional probability that the B layer is generated after the pair of layers AA, and so on.

In the Hendricks-Teller structure,[4] the probability that a layer is present in a certain position depends on the neighboring layers as well as the abundance of the layer in question. By changing the value of the parameter q measuring the correlation among neighboring layers, it is possible to conveniently obtain a variety of different arrangements ranging from the alternating checkerboard-like periodic pattern to the phase segregated case. For a positive value of q, the same kind of layers tend to stack side by side; thus, as q increases, the number of the interfaces between the layers A and B decreases. For $q = 1/4$, the system becomes a phase separated single heterostructure where every layer of material A (B) is attached to material A (B), except at the only interface. The case $q = 0$ corresponds to the completely random SL, which has been studied in detail in Ref. 15. For a negative value of q, layers A and B tend to stack in an alternating fashion, and as q decreases the system becomes closer to a periodic SL which is attained for $q = -1/4$ (with $f_A = f_B = 1/2$). In summary, a negative q encourages alternation among layers while a positive q favors phase segregation.

The study of quasicrystalline diffraction patterns has been partly responsible for a renewal of interest in the HT model.[16] Several variations of it have been considered. In one of them, the independent random variables are the spacings between the planes (or scatterers). In another one, the planes are first periodically spaced and then randomly displaced. This difference is not physically significant from the point of view of speckle.[14,16]

III. *N*-STATE MARKOV SUPERLATTICES

Let us now consider a different type of SL with a controlled degree of randomness. It is modeled after the so-called Markov property in the theory of fluctuations, noise, and stochastic processes.[17] In fact, the subclass of Markov systems is by far the most important stochastic process in physics and chemistry.[5,18] Since SL's based on this structure are not well known in the multilayer community, it is worthwhile to explain the origin and motivation for this kind of system, and a few results useful for calculations in the next few sections.

The oldest and best known example of a Markov process in physics is Brownian motion. If a series of observations of the same Brownian particle gives a sequence of locations $\mathbf{r}_1$, $\mathbf{r}_2$, . . . , $\mathbf{r}_n$, $\mathbf{r}_{n+1}$, . . . , each displacement $\boldsymbol{\delta}_{n+1} = \mathbf{r}_{n+1} - \mathbf{r}_n$ is affected by chance, and its probability distribution only depends on $\mathbf{r}_n$ and is independent of the previous history $\mathbf{r}_{n-1}$, $\mathbf{r}_{n-2}$, ... Thus, on the sequence of time intervals imposed by a particular experiment, the position and the velocity of the particle are Markov processes. This picture forms the basis of the theory of Brownian motion. Other examples of Markov processes are the radioactive nuclear decay, the escape of gas molecules through a small leak, the destruction of cells by radiation, and the emission of light by excited atoms. In all of them, on the sequence of time intervals imposed by a series of measurements, the state of the system at time t_n, *only* depends on the state at time

t_{n-1} and is independent of the states at all previous times t_{n-2}, t_{n-3}, ... Also, the concept of a Markov process is not restricted to one-component processes but applies to m components as well. The three velocity components of a Brownian particle and the m chemical components of a reacting mixture are two examples.

In the previous paragraphs, the word "process" was used in its standard physics manner, i.e., usually referring to the time evolution of a system. However, sometimes the underlying evolving variable is not time but space. An example is given by the following Markov process: the loss of cosmic ray electrons in an absorbing material, the traversed thickness playing the role usually assigned to time. Here we also consider space (along the growth direction) in a similar manner. Also, in this paper as in most experiments, we build our structures one layer at a time. Starting with layer X, we add the next layer, either X or Y, according to the probabilities Q_{XX} and Q_{XY}. Thus, in a Markov SL the addition of any new layer only depends on the type of layer (or block of layers) most recently added and not on the previous ones.

We now proceed to describe Markov SL's with short-range correlations in the sequence of constituent layers. Specifically, we consider versions of the quasicrystalline and Thue-Morse SL's lacking long-range coherence. The deterministic quasicrystalline or Fibonacci sequence has long-range order manifested by the presence of a dense set of Bragg peaks in its structure factor.[19] It is generated by iterating the substitution rules $A \rightarrow AB$ and $B \rightarrow A$, so only three possible neighboring pairs of layers AA, AB, and BA (three states) are present, and the BB pair never appears. In order to preserve this short-range ordering, we generate a Markov sequence based on it, by using the following straightforward three-state Markov chain rules: (i) layer B is generated with probability one after the pair of layers AA , i.e., $P_{(AA|B)} = 1$, because AAA is a forbidden arrangement in the original system with long range order; (ii) layer A is generated with probability one after AB, i.e., $P_{(AB|A)} = 1$, because BB is not allowed in the original structure with long-range order; and (iii) $P_{(BA|A)} = \tau^{-1}$ and $P_{(BA|B)} = \tau^{-2}$, respectively, where $\tau = (\sqrt{5}+1)/2$. The last step is the only one that introduces randomness in this structure. Therefore, the probability of occurrence (i.e., frequency) for the layers themselves are $f_A = \tau^{-1}$ and $f_B = \tau^{-2}$. All these probabilities also apply to the original deterministic structure with long-range order. However, the Markov sequences generated according to the above probabilistic rules lack long-range coherence.

The TM chain[8,20] is a deterministic sequence that has a degree of order intermediate between the quasiperiodic and random cases. In spite of its aperiodicity, the TM Fourier spectrum exhibits very prominent peaks that would be absent in a random sequence. It is the scaling invariance of the TM chain (periodicity on a logarithmic scale) which produces long-range correlations. Many different prescriptions can generate the TM sequence, the simplest one is through the substitution rules: $A \rightarrow AB$ and $B \rightarrow BA$. In this sequence, the adjacent pairs AA, AB, BA, and BB (four states) appear with equal probability, and blocks AAA and BBB are not allowed.

We can generate a partially disordered structure, which preserves the TM short-range arrangement among adjacent layers, by following the simple rules: (i) layer B (A) is added after layer AA (BB) with probability one, i.e., $P_{(AA|B)} = 1$ and $P_{(BB|A)} = 1$; (ii) add layers A and B, with equal probabilities, after the pairs of layers AB and BA, e.g., $P_{(AB|A)} = 1/2$ and $P_{(BA|A)} = 1/2$. Note that $f_A = f_B = 1/2$ holds in the partially ordered TM sequences.

IV. BACKSCATTERING RATE OF PHONONS

In a recent paper, we have shown that the transmission rate, localization length, and transmission fluctuations of phonons in random SL's are derived from the backscattering rate of phonons due to mass density fluctuations in SL's.[15] Incorporating all of the forward scattering contributions, we can relate the scattering rate to the ensemble average of the squared SL structure factor I_s defined by $I_s = \langle |S_N|^2 \rangle / N$, where

$$S_N = \sum_{j=0}^{N} (-1)^j \exp\left(-i \sum_{m=0}^{j} \theta_m\right) \tag{4}$$

is the structure factor of a SL ($\theta_0 = 0$). Here N is the number of A and B blocks (several consecutive identical A layers define an A block, or block A) in the SL and $N-1$ is the number of interfaces between blocks A and B. We use the words "layer" and "block" in the following way: an elementary or basic layer made of material A, with thickness d_A, is called an A layer or layer A. Also, n consecutive A layers form an A block, or block A. The same notation applies to B. In Eq. (4), θ_m denotes twice the phase factor which phonons gain in passing through the mth block of a SL consisting of a disordered sequence of layers A and B. More explicitly, starting from an A block, $\theta_{2j-1} = 2k_A D_{2j-1}$ and $\theta_{2j} = 2k_B D_{2j}$, ($j = 1, 2, \ldots$) where k_A and k_B are the wave numbers of phonons in A and B layers and D_{2j-1} and D_{2j} are the thicknesses of the $(2j-1)$th and $2j$th blocks in a random SL consisting of A and B layers, respectively. (Note that $D_{2j-1} = (n_A)_{2j-1} d_A$ and $D_{2j} = (n_B)_{2j} d_B$, where $(n_A)_{2j-1}$ and $(n_B)_{2j}$ are the number of consecutive A (B) layers making the $(2j-1)$th [$(2j)$th] block and d_A and d_B are the thicknesses of the basic or elementary A and B layers.) The interface between two consecutive identical layers (e.g., the interface between the A and A layers in an AA block) does not produce any scattering, therefore, the only relevant interfaces are between different types of layers or the interfaces between A and B blocks.

Now we calculate the intensity I_s for the partially ordered SL's. Assuming N is an even number ($N = 2n$), we can rewrite Eq. (4) as

$$S_N = \sum_{j=1}^{n} [1 - \exp(-i\theta_{2j})] \exp\left(-i \sum_{m=1}^{2j-1} \theta_m\right). \tag{5}$$

Thus, we obtain

$$|S_N|^2 = \sum_{j=1}^{n} (1 - e^{-i\theta_{2j}}) - \sum_{j=2}^{n} \sum_{m=1}^{j-1} (1 - e^{-i\theta_{2j}})(1 - e^{-i\theta_{2m}}) e^{-i(\theta_{2j-1}+\theta_{2j-2}+\cdots+\theta_{2m+1})} + \text{c.c.} \quad (6)$$

We consider the case where no correlation exists between the thicknesses of the adjacent blocks (this is valid for the case we are considering) and put

$$\langle \exp(-i\theta_{2j-1}) \rangle = \langle \exp(-2ik_A D_{2j-1}) \rangle \equiv \epsilon_A, \quad \langle \exp(-i\theta_{2j}) \rangle = \langle \exp(-2ik_B D_{2j}) \rangle \equiv \epsilon_B. \quad (7)$$

Now it is straightforward to derive the expression of I_s for $|\epsilon_A \epsilon_B| < 1$.[21] The result is

$$I_s = \text{Re}\left[\frac{(1-\epsilon_A)(1-\epsilon_B)}{1-\epsilon_A\epsilon_B}\right]. \quad (8)$$

To proceed further, we calculate ϵ_A and ϵ_B for any given partially random sequence of A and B layers. For the Hendricks-Teller model, we find the following averaged phase factors:

$$\epsilon_A = \frac{P_{AB}\, e^{-ia}}{1 - P_{AA}\, e^{-ia}}, \quad \epsilon_B = \frac{P_{BA}\, e^{-ib}}{1 - P_{BB}\, e^{-ib}} \quad (9)$$

and averaged block lengths

$$\langle D_{2j-1} \rangle \equiv \langle D_A \rangle = \frac{P_{AB}}{(1-P_{AA})^2}\, d_A, \quad \langle D_{2j} \rangle \equiv \langle D_B \rangle = \frac{P_{BA}}{(1-P_{BB})^2}\, d_B, \quad (10)$$

where $a = 2k_A d_A$ and $b = 2k_B d_B$. Similarly, for the three-state Markov SL with short-range quasicrystalline order we obtain

$$\epsilon_A = \frac{1}{\tau} e^{-2ia} + \frac{1}{\tau^2} e^{-ia}, \quad \epsilon_B = e^{-ib}, \quad (11)$$

and $\langle D_A \rangle = \tau d_A$ and $\langle D_B \rangle = d_B$. For the Markov TM SL

$$\epsilon_A = \frac{1}{2}(e^{-ia} + e^{-2ia}), \quad \epsilon_B = \frac{1}{2}(e^{-ib} + e^{-2ib}), \quad (12)$$

and $\langle D_A \rangle = 3d_A/2$ and $\langle D_B \rangle = 3d_B/2$.

The explicit expression of $I_s \equiv I_s^{\text{HT}}$ for SL's based on HT model (with $f_A = f_B = 1/2$) is

$$I_s^{\text{HT}} = \frac{2(1+4q)(\cos\phi - \cos\delta)^2}{(1+4q)^2(\cos\phi - \cos\delta)^2 + (1-4q)^2 \sin^2\phi}, \quad (13)$$

where $\phi = (a+b)/2$ and $\delta = (a-b)/2$. Also we find $I_s \equiv I_s^{M-\text{QC}}$ and $I_s \equiv I_s^{M-\text{TM}}$ for Markov QC and Markov TM SL's as

$$I_s^{M-\text{QC}} = \frac{(1-\cos a)(1-\cos b)}{\cos a + \tau\,[2 - \cos(a+b)] - \tau^2 \cos(2a+b)}, \quad (14)$$

$$I_s^{M-\text{TM}} = \frac{\frac{1}{2}(1-\cos a)(1-\cos b)(\cos a + \cos b + 5/2)}{1 + \cos^2\frac{a}{2}\cos^2\frac{b}{2} - \frac{1}{2}\,[\cos(a+b) + \cos(2a+b) + \cos(a+2b) + \cos(2a+2b)]}. \quad (15)$$

Now, according to our previous work,[15] the elastic backscattering rate of phonons due to mass-density fluctuations in random SL's is given in the Born approximation as

$$\Gamma(\omega) = \frac{c_A}{D_0} R^2 I_s, \quad (16)$$

where $D_0 = (\langle D_A \rangle + \langle D_B \rangle)/2 = L/N$ is the average thickness of one block in the system (L being the total length of the SL), and $R = (Z_A - Z_B)/(Z_A + Z_B)$ with $Z_i = \rho_i c_i$ ($i = A$ and B, and c_i is the sound velocity) is the amplitude reflection coefficient. Here we note that both the substrate and detector are assumed to be made of A material and the homogeneous system consisting of only A material is taken as the unperturbed system based on which the calculation of the phonon transmission rate is developed. Thus, D_0/c_A gives the average time for phonons to propagate through the length of a single block in the unperturbed structure.

V. PHONON TRANSMISSION RATE, LYAPUNOV EXPONENT, AND TRANSMISSION FLUCTUATIONS

In Ref. 15 we have derived a formula which relates the phonon backscattering rate to the transmission rate. Introducing a scaling parameter $t = (L/c_A)\Gamma = L/\ell$ ($\ell = c_A/\Gamma$ is the elastic mean free path of backscattering), the average transmission rate $\langle T \rangle$ is given by

$$\langle T\rangle = \int_0^\infty \frac{2\pi\lambda \tanh \pi\lambda}{\cosh \pi\lambda} \exp\left[-\left(\frac{1}{4}+\lambda^2\right)t\right] d\lambda \ . \quad (17)$$

This formula was originally derived in the study of the electrical conductivity in one-dimensional disordered metals.[22]

The Lyapunov exponent γ, defined by[23]

$$\gamma = -\lim_{L\to\infty} \langle \ln T\rangle/2L, \quad (18)$$

is an important quantity which provides the phonon localization length $\xi = \gamma^{-1}$. The Lyapunov exponent is the logarithmic decrement of the transmission coefficient averaged over the realizations of disorder. It can be proved that $\gamma = \Gamma/(2c_A) = 1/2\ell$, so γ is directly related to the structure factor or I_s.[15] Also, the standard deviation of the transmission

$$\Delta T = (\langle T^2\rangle - \langle T\rangle^2)^{1/2} \quad (19)$$

is calculated from Eq. (14) by employing the relation[24]

$$\langle T^2\rangle = -\frac{d\langle T\rangle}{dt} \ . \quad (20)$$

In the next section, we will present comparisons between our analytical and numerical results for a variety of SL's. It is important to point out that the plots presented below are not "fingerprints" (or speckle patterns) of specific configurations of disorder but averages over many realizations of disorder. The term speckle pattern refers to the complex interference pattern in the transmitted intensity as a function of frequency (or the outgoing direction). Each realization of a random medium (i.e., each sample of the statistical ensemble) displays its own pattern, or fingerprint, which reflects the specific arrangement of the inhomogeneities (e.g., impurities) in that sample. This phenomenon, called "speckle pattern," is familiar in optics[14] and it refers to the intensity pattern formed on a screen by light reflected from a rough surface. The detailed study, with experimental predictions, of the phonon spectroscopy analog of these fingerprints will be presented elsewhere.

The expression "universal-transmission fluctuations" clearly does not refer to the phonon analog of "universal conductance fluctuations" but to the fact that different realizations of disorder have fluctuations which fall on the very same *universal* curve for the standard deviation versus average transmission. In fact, we do obtain, analytically and numerically (for a variety of SL's), a universal curve (ΔT versus $\langle T\rangle$) for the transmission fluctuations. Also, universal conductance fluctuations are not directly related to localization, while our focus here is on localization. Finally, it has been pointed out that the notation universal conductance fluctuations is a misnomer because it refers to a sample-dependent, and therefore nonuniversal, fingerprint. Currently, they are more appropriately denoted by the term "reproducible conductance fluctuations."

VI. COMPARISON BETWEEN ANALYTICAL AND NUMERICAL RESULTS

A. Hendricks-Teller model

Figures 1–5 present calculations for the quantities described above, obtained by using two very different approaches. In one of them, we use the analytical expressions presented in this paper. In the other one, we use the transfer matrix method for numerical calculations. In the latter method, the displacement and stress fields associated with the incident and transmitted waves are connected to each other by the product of the transfer matrices describing the physical properties of each constituent layer of the SL. The transmission rate is expressed in terms of elements of the product of the transfer matrices, by imposing proper boundary conditions on the incoming and outgoing waves. Readers interested in a pedagogical introduction to transfer matrices and other related techniques are referred to Ref. 23.

In order to verify the accuracy of our predictions, it is important to compare the results obtained from these two quite different approaches.

Figures 1(a)–1(c) plot $\langle T\rangle$ versus frequency for the Hendricks-Teller model with $f_A = f_B = 1/2$ and for $q = 1/8$, 0, and $-1/8$. For $q = 1/8$, the same kind of layers tend to stack side by side; $q = 0$ corresponds to the completely random SL, and for $q = -1/8$, layers A and B tend to stack alternatively. For $q = 1/4$ the system is phase segregated with a single heterostructure and the transmission rate becomes a constant independent of the phonon frequency. For $q = -1/4$ the system is a periodic SL and sharp dips in transmission occur due to the Bragg reflection of phonons. Figures 1(a)–1(c) properly reflect the features characteristic of these SL systems with a highly controlled degree of disorder. To plot these figures we have chosen 34-Å-thick GaAs and AlAs as the A and B layers, respectively. The average transmission reveals various structures including sharp enhancements and dips. The former, with $\langle T\rangle \simeq 1$, are the resonances which occur for phonons whose wavelengths match the thicknesses of A and B layers. More explicitly, the resonances occur for $\cos a = 1$ and $\cos b = 1$, or equivalently at $\nu = \nu_{i,n}^{(R)} = nc_i/2d_i$ ($i = A$ or B, and n is an integer). This can be seen from Eq. (13) by noting that $(\cos\phi - \cos\delta)^2 = (1-\cos a)(1-\cos b)$. Numerically, the resonance frequencies are $\nu_{A,n}^{(R)} = 490 \times n$ GHz and $\nu_{B,n}^{(R)} = 582 \times n$ GHz.

The dips in $\langle T\rangle$ are due to *constructive interference* of backscattered phonons. In the HT SL's the minima of $\langle T\rangle$ are realized at the frequencies $\nu = \nu_n^{(B)} \equiv n/2(d_A/c_A + d_B/c_B)$. These are the Bragg frequencies (numerically $\nu_n^{(B)} = 266 \times n$ GHz) in the periodic SL's consisting of an alternating stacking of A and B layers. It should be noted that $\langle T\rangle$ is monotonically decreasing as t ($\propto \Gamma \sim I_s$) increases, and I_s takes its maximum value for $\sin\phi = 0$ or $\nu = \nu_n^{(B)}$ [see Eq. (13)]. We find that the overall agreement between the analytical and numerical results is excellent, even though we observe large fluc-

tuations in $\langle T \rangle$. These fluctuations are small only for T close to zero and unity and remain large even if we increase the system size, i.e., the phonon transmission is not a self-averaging quantity, as described in Refs. 24 and 25.

The frequency dependence of the Lyapunov exponent, which is proportional to I_s, is also plotted in Fig. 2 for $q = 1/8$, 0, and $-1/8$. At the resonances, γ vanishes because $I_s = 0$ and the phonons are delocalized. The maximum values $\gamma_{\max}$ of γ are achieved at the Bragg frequencies $\nu_n^{(B)}$. At these frequencies $I_s = 4/(1+4q)$ because $\sin\phi = 0$ and from Eq. (10)

$$D_0 = \frac{2}{1-4q}(f_A d_A + f_B d_B), \tag{21}$$

so $\gamma_{\max}$ are proportional to $(1-4q)/(1+4q)$. This explains the relative magnitudes of $\gamma_{\max}$ for different values of q shown in Fig. 2. We also note that in the present case, the localization lengths are longer than 3000 Å, which is much larger than the typical wavelength of 35 Å at a 1-THz frequency. Even under this condition, phonons in an infinite, partially ordered SL are localized except at resonance frequencies due to the coherent interference of backscattered waves.[26]

Figure 3 exhibits ΔT versus $\langle T \rangle$ plotted together for different values of q. It is important to emphasize that the data lie on a *universal* curve irrespective of the value of q (magnitude of the correlation) and also of the specific type of ordering of the SL. There is a certain amount of fluctuation in the data numerically computed via trans-

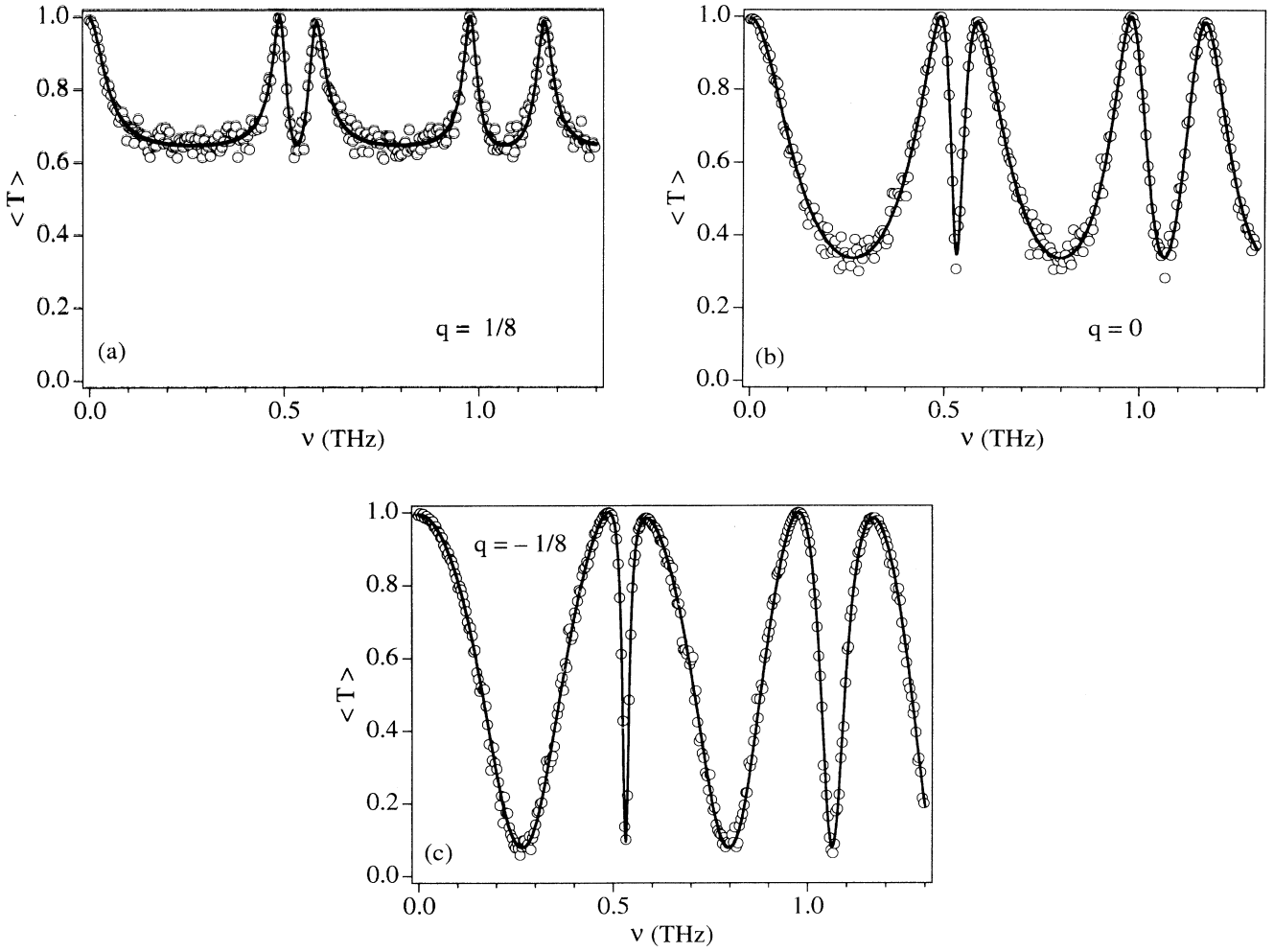

FIG. 1. Average phonon transmission rate $\langle T \rangle$ versus frequency ν for a Hendricks-Teller SL with 200 layers, $f_A = f_B = 1/2$, for (a) $q = 1/8$, (b) $q = 0$, and (c) $q = -1/8$. These and the following figures consider 34-Å-thick GaAs (A) and AlAs (B) layers as the basic units for constructing the SL's. The continuous line is our analytical result while the open circles are obtained from a numerical calculation using transfer matrices and averaging over 100 realizations of disorder. The fluctuations in the average transmission are very small when $\langle T \rangle \sim 1$ and become much larger for the intermediate values of $\langle T \rangle$, i.e., for $0.2 \lesssim \langle T \rangle \lesssim 0.6$. Note also that the amount of transmitted phonons decreases significantly with decreasing q. This can be understood as follows: Similar kinds of layers tend to stack together when $q = 1/8$, thus reducing the number of interfaces with an acoustic mismatch, which are the scatterers. For $q = -1/8$, layers A and B tend to stack alternatively increasing the number of interfaces (i.e., scatterers).

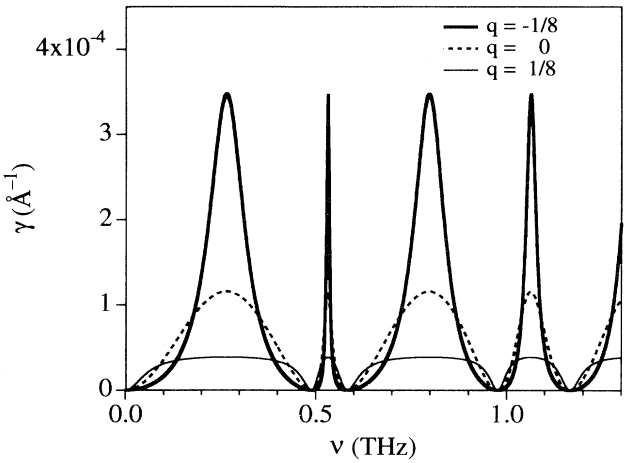

FIG. 2. Lyapunov exponent γ (the inverse of the localization length ξ) versus phonon frequency ν, for HT SL's with $q = 1/8$ (thin solid line), 0 (dashed line), and $-1/8$ (bold solid line). At the resonance frequencies $\nu_{i,n}^{(R)}$, γ vanishes, and at the Bragg frequencies $\nu_n^{(B)}$, γ takes its maximum value. The localization lengths are about two orders of magnitude larger than the typical wavelength of 35 Å at a 1-THz frequency. Note that the larger the number of interfaces (i.e., for $q = -1/8$), the sharper the peaks in the Lyapunov exponent as described in the text.

fer matrices (shown as scattered points in the figure). This fluctuation, however, decreases when the average is taken over an ensemble consisting of a larger number of SL's. We have also explicitly shown (see Fig. 3) that the standard deviation ΔT vanishes for $\langle T \rangle = 1$ and 0, monotonically increases in the range $\langle T \rangle \lesssim 0.4$, and monotonically decreases in the range $\langle T \rangle \gtrsim 0.4$.

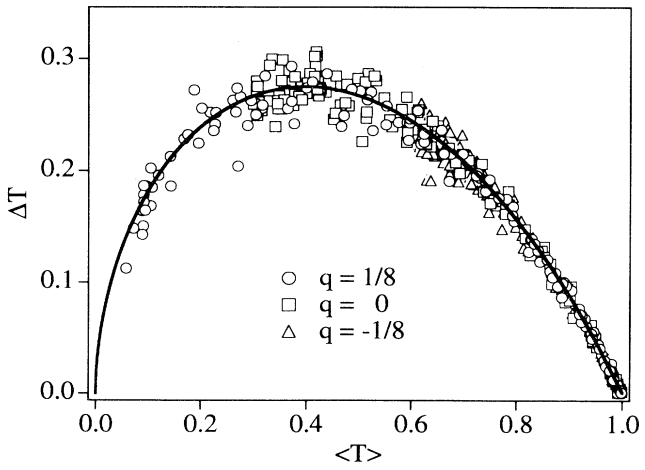

FIG. 3. Standard deviation of the phonon transmission rate $\Delta T = (\langle T^2 \rangle - \langle T \rangle^2)^{1/2}$ versus $\langle T \rangle$, for the same HT SL as in Figs. 1 and 2. The continuous line is the theoretical prediction, obtained from Eqs. (17) and (20). The points are computed using the transfer matrix method and an ensemble average over $N_{\rm av} = 100$ realizations of disorder. Fluctuations in the points diminish for increasing values of $N_{\rm av}$.

B. QC and TM Markov superlattices

The average transmission rate versus frequency for the Markov versions of the quasicrystalline and TM SL's are plotted in Fig. 4 together with the transmission rate of the original QC and TM SL's with long-range deterministic order. The basic layers A and B assumed here are the same ones used for the HT model. In the regular QC SL considered here, the transmission dips occur at frequencies $\nu_{m,n} \equiv (m + n\tau)v/(2\tau^2 d)$, where m and n are integers, v is the average sound velocity in the SL, and $d = \tau d_A + d_B$. When m and n are neighboring Fibonacci numbers, i.e., $(m, n) = (F_{p-1}, F_p)$ where $F_{p+1} = F_p + F_{p-1}$ and $(F_0, F_1) = (0, 1)$, $\nu_{m,n} = \nu_p \equiv \tau^{p-2} v/2d$ holds and a major dip is realized. We have indicated in Fig. 4(a) the set of integers (m, n) for several major dips. In the regular TM SL we study, large dips in

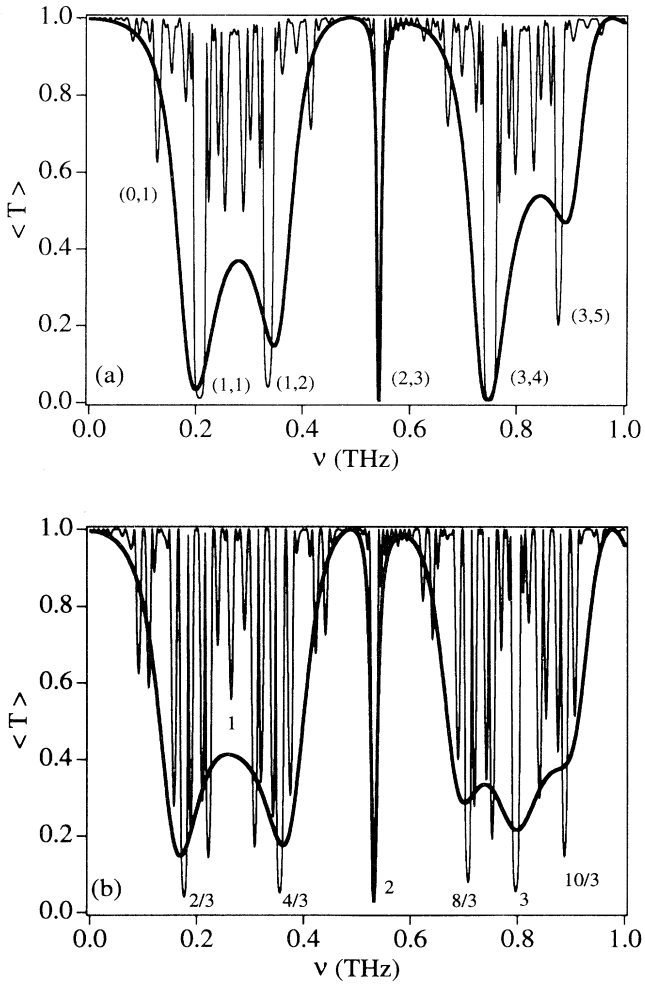

FIG. 4. Average transmission rate $\langle T \rangle$ versus frequency ν for the Markov versions (bold solid lines) of the (a) QC and (b) TM SL's. Also plotted by thin solid lines are the transmission rates for the original, deterministic (a) QC and (b) TM SL's with 55 and 64 layers, respectively. The physical parameters assumed here are the same ones used for the HT SL. Several major dips in $\langle T \rangle$ are labeled (see the text).

transmission happen at frequencies ν_n and $\nu_{n/3} = \nu_n/3$, where $\nu_n = \nu_n^{(B)}$. We have labeled in Fig. 4(b) the indices of the frequencies for several major dips. We see that the small dips exhibiting the self-similar structures characteristic of the QC SL (Ref. 2) are smeared out in the three-state QC Markov SL, producing rather broad transmission dips. Similar results can be seen for the four-state TM Markov case.

Figures 5–7 show the results for the three-state QC and four-state TM Markov SL's corresponding to Figs. 1–3 of the HT model. In Fig. 5, the average transmission rate $\langle T \rangle$ versus frequency ν is presented and the agreement between the analytically derived results and the numerical calculations is excellent. The transmission fluctuations are large for an intermediate value of $\langle T \rangle$ as in the case of the HT model. The Lyapunov exponent γ versus frequency is presented in Fig. 6. The explicit expressions

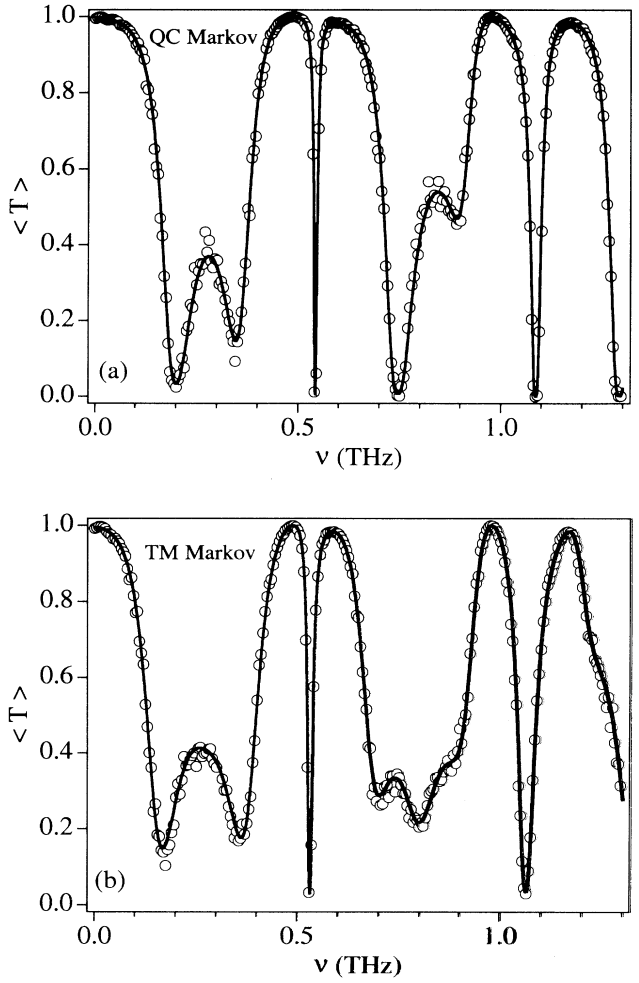

FIG. 5. Average transmission rate $\langle T \rangle$ versus frequency ν of (a) QC and (b) TM Markov SL's. The continuous lines are the analytical calculations and the open circles are the numerical results for the (a) three-state QC and (b) four-state TM Markov SL's. The results shown are those averaged over an ensemble of 100 random SL's. Each random SL consists of 200 basic A and B layers.

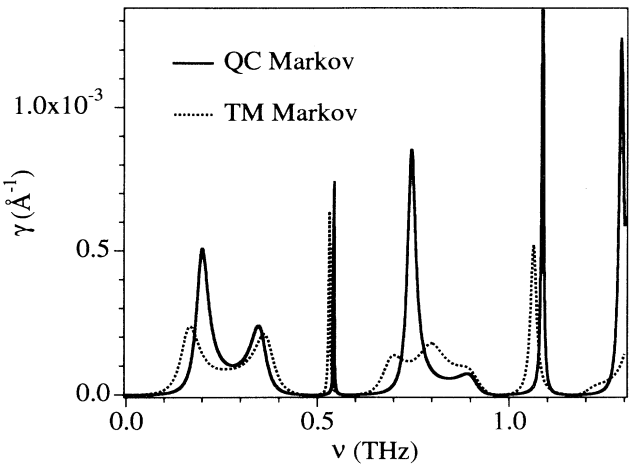

FIG. 6. Analytically calculated Lyapunov exponent γ versus frequency for the QC Markov (solid line) and TM Markov (dashed line) SL's.

of I_s ($\propto \gamma$) for the QC Markov and TM Markov SL's are given by Eqs. (14) and (15). From these equations we see that the resonances ($\gamma = 0$) in these systems occur at the same frequencies $\nu_{i,n}^{(R)}$ (satisfying $\cos a = 1$ or $\cos b = 1$) as in the HT SL's. Unfortunately, however, we could not find any simple explicit analytical expression for the frequencies at which the maximum values of γ are attained. The standard deviation of the phonon transmission rate ΔT versus $\langle T \rangle$ is shown in Fig. 7. In this figure the continuous line is the theoretical prediction, which agrees well with the numerical points obtained by averaging over 100 realizations of disorder. Here it should be noted that the analytical results for both $\langle T \rangle$ and ΔT are functions of only the scaling parameter $t = L/\ell$, the system size di-

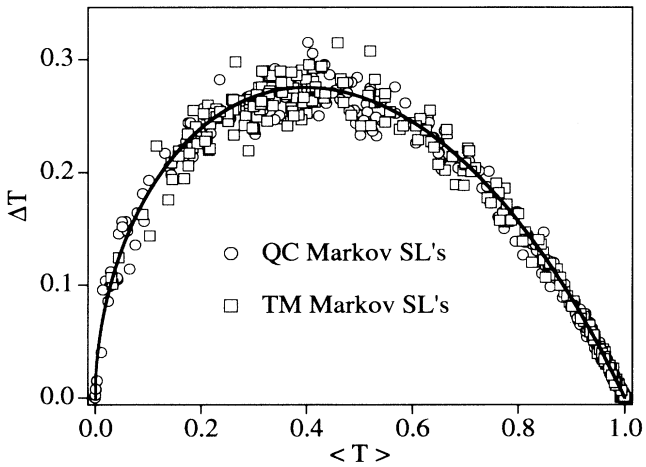

FIG. 7. Standard deviation of the phonon transmission rate ΔT versus average transmission $\langle T \rangle$. The continuous line is the theoretical prediction. Open circles and squares are the numerical results for the Markov versions of the QC and TM SL's obtained from the transfer matrix method by averaging 100 realizations of disorder.

vided by the mean-free path. Thus, ΔT versus $\langle T \rangle$ does not depend on the structures of the SL's and the analytical curve in Fig. 7 is identical to that in Fig. 3 for the HT model.

VII. CONCLUSIONS

In summary, we have derived analytical expressions of I_s, the average phonon intensity reflected from the interface layers, for several SL's with varying degrees of short-range correlation. From I_s, we derive the localization lengths, transmission rate, and transmission fluctuations, all of which coincide well with the numerical results obtained from the transfer matrix method.

In the SL's based on the HT model, the introduction of correlations among neighboring layers drastically changes the behavior of the phonon transmission. In particular, the rate of transmitted phonons decreases significantly with decreasing q. Also, the fluctuations in the average transmission are very small close to $\langle T \rangle \sim 1$ and $\langle T \rangle \sim 0$, and become much larger for intermediate values of $\langle T \rangle$.

The introduction of disorder in the QC and TM SL's produces a decrease in the phonon long-range coherence which is reflected in the smearing out of small peaks in I_s and equivalently the smearing out of the small dips in the transmission rate. In spite of these quantitative differences in the fine structure, the overall qualitative behavior is still the same as in the ordered case in the sense that it still exhibits pronounced peaks and dips in approximately the same locations as in the original deterministic SL's. Here we note, however, that the structure factors in the original, ordered QC and TM SL's have very sharp peaks at $\nu = \nu_p$ and $\nu = \nu_{n/3}$, respectively, which means that I_s grows in proportion to the system size or N at these frequencies. In the Markov SL's, which only preserve short-range QC or TM ordering, I_s remains finite on the entire frequency range of phonons, even if the system size is increased indefinitely.

We have obtained ΔT versus $\langle T \rangle$ through two different approaches. The data lie on a *universal* curve irrespective of the value of q (magnitude of the correlation) and of the specific type of ordering of the SL as demonstrated numerically for both HT SL's and two kinds of Markov SL's. This is because both $\langle T \rangle$ and ΔT are determined only by the magnitude of the elastic mean free path and the system size but does not depend explicitly on the details of the structure of random SL's.

One of the main findings of this work is that the loss of long-range order does not produce large qualitative changes in the overall structure of the phonon transmission rate, while it drastically affects its fine structure. At first sight, it might seem surprising to see that the very-short-range correlations among neighboring layers dominate the overall frequency-dependent transmission rate of the traveling phonons. By increasing the degree of ordering in the SL in a controlled manner, we find that the long-range ordering is responsible for the fine structure present in the transmission rate. Furthermore, this effect has been precisely quantified through the computation of Lyapunov exponents and other quantities useful for describing the localized character of the phonons. Moreover, we have applied these ideas to two families of SL's where the degree of order can be systematically changed in a convenient manner. Finally, we have applied the results derived here to several particular realizations of GaAs-AlAs SL's which are readily accessible experimentally. Thus, our predictions for the phonon universal transmission fluctuations can be tested using currently existing experimental techniques in phonon spectroscopy.

Finally, we note that a very interesting experiment has recently been done by Kono and Nakoda, which studies the localization properties of the third sound waves by directly measuring the transmission spectra in 1D random lattices.[27] The observed averaged transmissivity reveals the frequency dependence very similar to those given in Figs. 1(a)–1(c), i.e., the periodic oscillation characteristic of the presence of both resonances (enhancements in transmission) and localizations (dips in transmission) of the waves.

ACKNOWLEDGMENTS

The authors would like to thank T. Sakuma and R. Richardson for useful comments on the manuscript. This work is supported in part by the Special Grant-in-Aid for Promotion of Education and Science, in Hokkaido University Provided by the Ministry of Education, Science and Culture of Japan, a Grant-in-Aid for Scientific Research from the Ministry of Education, Science, and Culture of Japan (Grants Nos. 03650001 and 05650048), the Suhara Memorial Foundation, and the Iketani Science and Technology Foundation. F.N. acknowledges partial support from the NSF Grant No. DMR-90-01502, GE, and SUN microsystems.

[1] R. Merlin, IEEE J. Quantum Electron. **QE-24**, 1791 (1988).
[2] S. Tamura and J.P. Wolfe, Phys. Rev. B **36**, 3491 (1987); D.C. Hurley, S. Tamura, J.P. Wolfe, K. Ploog, and J. Nagle, *ibid.*, **37**, 8829 (1988).
[3] Y. Zhu, N. Ming, and W. Jiang, Phys. Rev. B **40**, 8536 (1989).
[4] S. Hendricks and E. Teller, J. Chem. Phys. **10**, 147 (1942).
[5] D. Isaacson and R. Madsen, *Markov Chains: Theory and Applications* (Wiley, New York, 1976).
[6] R. Merlin, K. Bajema, J. Nagle, and K. Ploog, J. Phys. (Paris) Colloq. **48**, C5-503 (1987).
[7] R. Merlin, K. Bajema, R. Clarke, F.Y. Juang, and P.K. Bhattacharya, Phys. Rev. Lett. **55**, 1768 (1985).
[8] S. Tamura and F. Nori, Phys. Rev. B **38**, 5610 (1988).
[9] V. Narayanamurti, H.L. Störmer, M.A. Chin, A.C. Gossard, and W. Wiegmann, Phys. Rev. Lett. **43**, 2012 (1979).
[10] O. Koblinger, J. Mebert, E. Dittrich, S. Döttinger, W. Eisenmenger, P.V. Santos, and L. Ley, Phys. Rev. B **35**, 9372 (1987).

[11] D.C. Hurley, S. Tamura, J.P. Wolfe, and H. Morkoc, Phys. Rev. Lett. **58**, 2446 (1987); S. Tamura, D.C. Hurley, and J.P. Wolfe, Phys. Rev. B **38**, 1427 (1988).
[12] P.V. Santos, J. Merbert, O. Koblinger, and L. Ley, Phys. Rev. B **36**, 1306 (1987).
[13] S. Washburn and R.A. Webb, Adv. Phys. **35**, 375 (1986); A.G. Aronov and Yu.V. Sharvin, Rev. Mod. Phys. **59**, 755 (1987).
[14] J.W. Goodman, in *Laser Speckle and Related Phenomena*, 2nd ed., edited by J.C. Dainty (Springer-Verlag, Berlin, 1984).
[15] N. Nishiguchi and S. Tamura, in *Proceedings of Phonon Scattering in Condensed Matter VII*, edited by R.O. Pohl (Springer-Verlag, Berlin, 1993), p. 427; N. Nishiguchi, S. Tamura, and F. Nori, Phys. Rev. B **48**, 2515 (1993).
[16] A. Garg and D. Levine, Phys. Rev. Lett. **60**, 2160 (1988); **63**, 1439 (1989).
[17] P. Hoel, S. Port, and C. Stone, *Introduction to Stochastic Processes* (Houghton, Boston, 1972).
[18] N.G. Van Kampen, *Stochastic Processes in Physics and Chemistry* (North-Holland, Amsterdam, 1981).
[19] D. Levine and P. J. Steinhardt, Phys. Rev. B **34**, 596 (1986).
[20] Z. Cheng, R. Savit, and R. Merlin, Phys. Rev. B **37**, 4375 (1988).
[21] S. Tamura and F. Nori, Phys. Rev. B **41**, 7941 (1990).
[22] A.A. Abrikosov and I.A. Ryzhkin, Adv. Phys. **27**, 147 (1978).
[23] See, for example, I.M. Lifshitz, S.A. Postur, and E. Yankovsky, *Introduction to the Theory of Disordered Systems* (Wiley, New York, 1988).
[24] A.A. Abrikosov, Solid State Commun. **37**, 997 (1981).
[25] P.W. Anderson, D.J. Thouless, E. Abrahams, and D.S. Fisher, Phys. Rev. B **22**, 3519 (1980).
[26] K. Ishii, Prog. Theor. Phys. Suppl. **53**, 77 (1973).
[27] K. Kono and S. Nakada, Phys. Rev. Lett. **69**, 1185 (1992).